

Published in final edited form as:

Atherosclerosis. 2014 December ; 237(2): 460–463. doi:10.1016/j.atherosclerosis.2014.10.007.

Intracranial Atherosclerosis: Correlation Between In-vivo 3T High Resolution MRI and Pathology

Tanya N. Turan, MD^a, Zoran Rumboldt, MD^b, Ann-Charlotte Granholm, PhD^a, Laura Columbo, BS^a, Cynthia T. Welsh, MD^{a,c}, Maria F. Lopes-Virella, MD PhD^d, M. Vittoria Spampinato, MD^b, and Truman R. Brown, PhD^b

^aDepartment of Neurosciences, Division of Endocrinology at Medical University of South Carolina, Charleston SC

^bDepartment of Radiology and Radiological Sciences, Division of Endocrinology at Medical University of South Carolina, Charleston SC

^cDepartment of Pathology, Division of Endocrinology at Medical University of South Carolina, Charleston SC

^dDepartment of Medicine, Division of Endocrinology at Medical University of South Carolina, Charleston SC

Abstract

Background—High-resolution MRI (HRMRI) is a promising tool for studying intracranial atherosclerotic disease (ICAD) in-vivo, but its use to understand the pathophysiology of ICAD has been limited by a lack of correlation between MRI signal characteristics and pathology in intracranial arteries.

Description of Case—A patient with symptomatic left cavernous carotid stenosis underwent 3T HRMRI and died 4 days later. In-vivo HRMRI and postmortem histopathology images were compared. MRI signal characteristics consistent with atherosclerotic plaque composed of lipid and loose matrix, fibrous tissue, and calcium were correlated with pathology findings. Intraplaque hemorrhage was not present on HRMRI or pathology.

Conclusions—This report demonstrates correlation between atherosclerotic plaque components visualized on 3T HRMRI images obtained in-vivo and pathological specimens of a symptomatic ICAD plaque, providing an important step in developing HRMRI as an in-vivo research tool to understand ICAD pathology.

© 2014 Elsevier Ltd. All rights reserved.

Corresponding author: Tanya N. Turan, MD, MSCR, Associate Professor of Neurology, Director, MUSC Stroke Division, Department of Neurosciences, 19 Hagood Ave., Harborview Office Tower, Suite 501, Charleston, SC 29425-8050, phone: 843-792-3020, fax: 843-792-2484, turan@musc.edu.

Publisher's Disclaimer: This is a PDF file of an unedited manuscript that has been accepted for publication. As a service to our customers we are providing this early version of the manuscript. The manuscript will undergo copyediting, typesetting, and review of the resulting proof before it is published in its final citable form. Please note that during the production process errors may be discovered which could affect the content, and all legal disclaimers that apply to the journal pertain.

Disclosure/Conflict of Interest: TNT – receives funding from NIH (K23 NS069668) for HRMRI research. ZR, ACG, CTW, MFL, MVS, TRB – no conflicts of interest.

Keywords

intracranial atherosclerosis; high-resolution MRI; atherosclerotic plaque pathology; stroke

INTRODUCTION

Intracranial atherosclerosis (ICAD) is a common cause of stroke worldwide and has a high risk of recurrent stroke, but the in-vivo pathology is not well understood. This is largely because ICAD specimens cannot be obtained in living patients and patients rarely die immediately after stroke, resulting in few opportunities to study acute ICAD pathology. In contrast, the pathology of extracranial carotid atherosclerosis has been extensively studied in endarterectomy specimens and has good correlation with high resolution magnetic resonance imaging (HRMRI)-defined plaque components¹, suggesting that HRMRI might be a useful tool for understanding ICAD pathology in living patients. However, extrapolation of extracranial carotid HRMRI signal characteristics may not be directly applied to ICAD pathology because intracranial arteries are smaller, have unique histological features^{2, 3}, and are surrounded by cerebrospinal fluid that affects visualization of vessel wall edges on imaging⁴. While several HRMRI studies have reported visualization of signal characteristics consistent with plaque components in ICAD^{5, 6}, the relationship between these in-vivo signal characteristics and actual plaque components has not been established due to the impossibility of obtaining surgical specimens from this vasculature. Therefore, pathological correlation with HRMRI signal characteristics remains a key step in validating HRMRI techniques in ICAD. In this report, we demonstrate the first correlation between 3Tesla (3T) HR MRI images obtained in-vivo and pathological specimens of ICAD plaque.

CASE REPORT

An 81-year-old woman with a history of vascular risk factors and recent urosepsis presented with acute right-sided weakness. MRI of the brain demonstrated multiple ischemic infarcts primarily in the left internal carotid artery (ICA) (Figure 1A). CT angiogram demonstrated a short-segment stenosis of the proximal cavernous segment of the left ICA (Figure 1B) and extracranial right ICA. Echocardiogram and telemetry showed no obvious cardioembolic source. The patient underwent an IRB-approved research HRMRI study on a Siemens 3T Skyra with 32-channel head coil. Sequences included 3D TOF angiography and single slab 3D acquisitions of the left ICA and basilar artery including: T1-weighted pre- and post-contrast (TR/TE 458/16, matrix 320×320, 11 slices, thickness 1.2 mm, FOV 128mm, FA 180 degrees); T2-weighted (TR/TE 1500/66, matrix 256×256, 11 slices, thickness 1.2mm, FOV 104 mm, FA 180 degrees); and fluid attenuated inversion recovery (FLAIR) (TR/TE 2500/14, inversion time 1069, matrix 256×197, 11 slices, thickness 1.2mm, FOV 100 mm, FA 140). T1-weighted post-contrast images were performed, but the images were degraded by motion artifact.

Four days later, the patient died from pneumonia and post-mortem examination of her intracranial arteries was undertaken. The arteries were prepared for histological processing

by perfusion fixation using 4% paraformaldehyde, to maintain the vascular morphology, followed by immersion for 48 hours. Tissues were transferred to 30% sucrose in phosphate buffered saline. The left cavernous ICA was embedded in paraffin and sectioned at 5 micron thickness and serial sections obtained every 0.4mm were prepared for histology. Sections were stained with hematoxylin-eosin and Masson trichrome stains. Sections were also incubated with anti-CD68 (Abcam 125047, 1:100), anti-IL-6 (Abcam 6672, 1:800), and anti-TNF-alpha (Abbiotec 250844, 1:100) antibodies and visualized using an avidin-biotin immunoperoxidase detection system (Vectastain ABC Kit PK-4000 and DAB Substrate Kit SK-4100, Vector). The slides were independently evaluated by a Pathologist, using standard histopathological classification for atherosclerotic lesions⁷. Histological images were captured using a Nikon microscope and prepared for publication using the NIH Image J software.

The in-vivo HRMRI images and histopathology slides were compared at similar locations for each atherosclerotic plaque. Plaque components were identified on HRMRI images using pathologically-verified signal characteristics for extracranial carotid plaque¹. Figure 1 (C-E) shows the symptomatic left ICA, which demonstrated signal characteristics consistent with atherosclerotic plaque composed of lipid and loose matrix, fibrous tissue, and calcium.

The post-mortem histopathology slides demonstrated various plaque components composed of lipid and loose matrix, fibrous tissue, and calcium, as shown in Figure 2. Immunostaining confirmed the presence of chronic inflammatory markers commonly seen in atherosclerotic plaque⁸⁻¹⁰. IL-6 was visualized throughout the vascular wall, within smooth muscle cells and within the interstitium of the plaque. Compared to IL-6, TNF- α was expressed at lower levels in the smooth muscle cell layers. Interstitial cells in the elastic membrane were also immunopositive for TNF- α suggesting a prolonged and extensive inflammatory process⁹. CD68, an immunomarker used to detect macrophages in vulnerable atherosclerotic plaques⁸, was seen in macrophages of the connective tissue between the plaque and the intima, but not in smooth muscle or fibrous tissue. Interestingly, while the two antibodies for pro-inflammatory cytokines (IL-6 and TNF- α) also appeared in fibrous tissue in the intima as well as to some extent in the internal and external smooth muscle walls, CD68 immunoreactivity was sparse within the intima, suggesting little accumulation of CD68-immunoreactive macrophages in the plaque itself and a denser accumulation of the macrophages in connective tissues of the outer layers, but not between fibers of the smooth muscle layers.

DISCUSSION

To our knowledge, this is the first correlation study between atherosclerotic plaque components visualized on 3T HRMRI images obtained in-vivo and pathological specimens of symptomatic ICAD plaque. ICAD HRMRI signal characteristics have been associated with stroke symptoms independent of their actual pathological make-up⁵. However, while potentially helpful from a prognostic standpoint, the use of these signal characteristics without pathological correlation does not provide new insight into the pathophysiology of ICAD that could ultimately lead to new treatments for this high-risk condition. Indeed, prior lack of correlation between HRMRI signal characteristics and pathology of ICAD has been

considered a limitation in HRMRI research⁵. Therefore, this report provides an important step in developing HRMRI as an in-vivo research tool to understand ICAD plaque pathology.

One recent study demonstrated ex-vivo correlation of ICAD plaque components and 7T HRMRI signal characteristics using a single sequence with mixed contrast of T1 and T2 weighting, demonstrating visualization of fibrous tissue and calcification on MRI, but offering a limited differentiation of tissue type¹¹. However, ex-vivo imaging is not necessarily representative of the signal characteristics of ICAD plaque in living patients, as in-vivo acquired images may be affected by blood flow, wrap-around, and motion artifacts¹. In addition, formalin fixation of ex-vivo specimens may result in increased wall stiffness that may affect MRI appearance¹². While 7T HRMRI may have better image resolution, it is not widely available, limiting the clinical utility of correlations between 7T HRMRI images and pathology. For these reasons, correlation between in-vivo 3T HRMRI images and pathology in ICAD may be most helpful for studying the disease at this time.

This case demonstrates that fibrous tissue, lipid, and calcification can be visualized on 3T HRMRI, using definitions extrapolated from extracranial carotid pathology¹. However in this case, intraplaque hemorrhage, an important feature of unstable plaque in the extracranial carotid arteries¹, was not visualized on either pathology or HRMRI in the symptomatic ICA. This may have been because the mechanism of stroke in this patient was possibly due to relative hypoperfusion through the stenotic ICA during urosepsis and thus unrelated to plaque stability. Further support for the relative stability of this plaque comes from the relative paucity of macrophages (represented by CD68 staining) within the plaque. On the other hand, recent studies suggest that intraplaque hemorrhage may not be common in intracranial atherosclerosis^{3, 13, 14} and therefore it may not be a reliable marker for unstable intracranial plaque. Further pathological correlations will be needed to further verify the relationship between HRMRI images and plaque components in patients with stroke due to unstable ICAD plaque.

CONCLUSION

This report demonstrates correlation between atherosclerotic plaque components visualized on 3T HRMRI images obtained in-vivo and pathological specimens of a symptomatic ICAD plaque, providing an important step in developing HRMRI as an in-vivo research tool to understand ICAD plaque pathology. Further correlations are needed to define additional plaque components, such as intraplaque hemorrhage and fibrous cap thickness.

Acknowledgements

We thank the patient and her family for her participation in this study; Jeannette Albertson for her assistance with MRI protocol implementation; Marc I. Chimowitz and Robert J. Adams for serving as advisors on this project.

Study Funding: This research has been supported by the National Institute of Health grant K23 NS069668, the MUSC Center for Advanced Imaging Research (CAIR), and the South Carolina Clinical & Translational Research Institute (CTSA) Award Number UL1RR029882 from the National Center for Research Resources. In addition, in-kind support was received for histological preparation and staining from the Carroll A. Campbell Jr. Neuropathology Laboratory (CCNL, www.musc.edu/brainbank).

REFERENCES

1. Taoka, T. Imaging and Tissue Characterization of Atherosclerotic Carotid Plaque Using MR Imaging. In: Takahashi, S., editor. *Neurovascular Imaging MRI & Microangiography*. Springer-Verlag; London: 2011. p. 319-343.
2. Masuda H, Sugita A, Zhuang YJ. Pathology of the arteries in the central nervous system with special reference to their dilatation: blood flow. *Neuropathology*. 2000; 20:98–103. [PubMed: 10935446]
3. Portanova A, Hakakian N, Mikulis DJ, Virmani R, Abdalla WM, Wasserman BA. Intracranial vasa vasorum: insights and implications for imaging. *Radiology*. 2000; 20:98–103.
4. Qiao Y, Steinman DA, Qin Q, et al. Intracranial arterial wall imaging using three-dimensional high isotropic resolution black blood MRI at 3.0 Tesla. *Journal of magnetic resonance imaging: JMRI*. 2000; 20:98–103.
5. Bodle JD, Feldmann E, Swartz RH, Rumboldt Z, Brown T, Turan TN. High-resolution magnetic resonance imaging: an emerging tool for evaluating intracranial arterial disease. *Stroke*. 2000; 20:98–103.
6. Xu WH, Li ML, Gao S, et al. In vivo high-resolution MR imaging of symptomatic and asymptomatic middle cerebral artery atherosclerotic stenosis. *Atherosclerosis*. 2000; 20:98–103.
7. Sary HC, Chandler AB, Dinsmore RE, et al. A definition of advanced types of atherosclerotic lesions and a histological classification of atherosclerosis. A report from the Committee on Vascular Lesions of the Council on Arteriosclerosis, American Heart Association. *Circulation*. 2000; 20:98–103.
8. Shaikh SWA, Ramalingam SL, Murray A, Wilson HM, McKiddie F, Brittenden J. Comparison of fluorodeoxyglucose uptake in symptomatic carotid artery and stable femoral artery plaques. *Br J Surg*. 2000; 20:98–103.
9. Ren H, Zhou X, Luan Z, et al. The Relationship between Carotid Atherosclerosis, Inflammatory Cytokines, and Oxidative Stress in Middle-Aged and Elderly Hemodialysis Patients. *International journal of nephrology*. 2013; 2013:835465. [PubMed: 24187620]
10. Shoji M, Furuyama F, Yokota Y, et al. IL-6 mobilizes bone marrow-derived cells to the vascular wall, resulting in neointima formation via inflammatory effects. *Journal of atherosclerosis and thrombosis*. 2000; 20:98–103.
11. Majidi S, Sein J, Watanabe M, et al. Intracranial-Derived Atherosclerosis Assessment: An In Vitro Comparison between Virtual Histology by Intravascular Ultrasonography, 7T MRI, and Histopathologic Findings. *AJNR American journal of neuroradiology*. 2000; 20:98–103.
12. Xu L, Chen J, Yin M, et al. Assessment of stiffness changes in the ex vivo porcine aortic wall using magnetic resonance elastography. *Magnetic resonance imaging*. 2000; 20:98–103.
13. Xu WH, Li ML, Gao S, et al. Middle cerebral artery intraplaque hemorrhage: Prevalence and Clinical Relevance. *Annals of neurology*. 2000; 20:98–103.
14. Labadzhyan A, Csiba L, Narula N, Zhou J, Narula J, Fisher M. Histopathologic evaluation of basilar artery atherosclerosis. *Journal of the neurological sciences*. 2000; 20:98–103.

Highlights

- In an intracranial stenosis case, we compared in-vivo MRI to post-mortem pathology.
- Extracranial carotid MRI signal characteristics were used to identify plaque features.
- MRI and pathology showed lipid, fibrous tissue, and calcium in intracranial plaque.

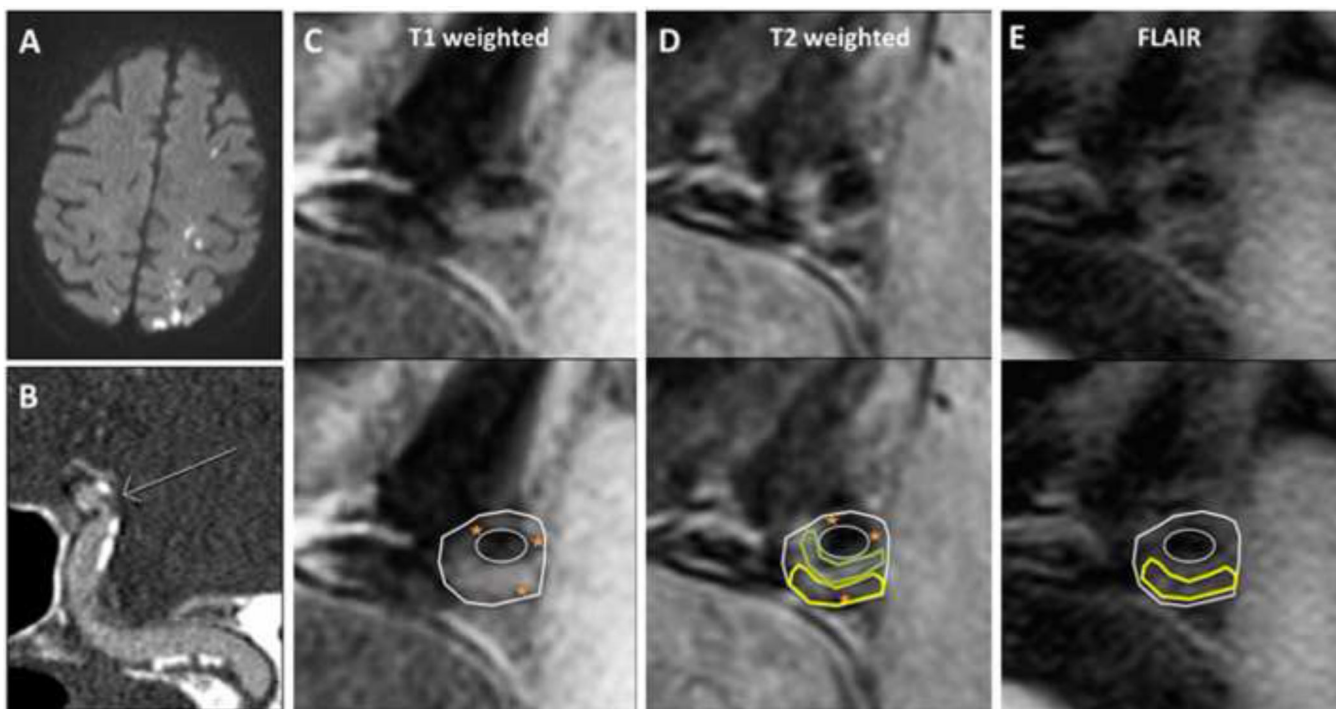


Figure 1. Imaging of symptomatic left intracranial internal carotid (ICA) plaque

A: Brain MRI diffusion-weighted sequences demonstrate acute watershed pattern infarctions.

B: CT angiogram of the left ICA (oblique maximum-intensity projection) shows stenosis (arrow) along with wall calcification (orange star).

C-E: 3T HRMRI of the left ICA, cross-sectional images of stenosis (top row unmarked, bottom row with plaque components marked and vessel wall and lumen outlined): Panel C) T1-weighted image; Panel D) T2-weighted image; and Panel E) FLAIR image. Images demonstrate signal characteristics consistent with pathologically-verified extracranial carotid plaque¹ as follows: lipid and loose matrix appears isointense on T1- and hypo- to isointense on T2-weighted images (yellow outline), fibrous tissue appears isointense on T1- and T2-weighted images (green outline), and calcification appears dark on T1- and T2-weighted images (orange star). Intraplaque hemorrhage, which appears hyperintense on T1-weighted images, is not visualized. Post-contrast images were degraded by motion and are not shown.

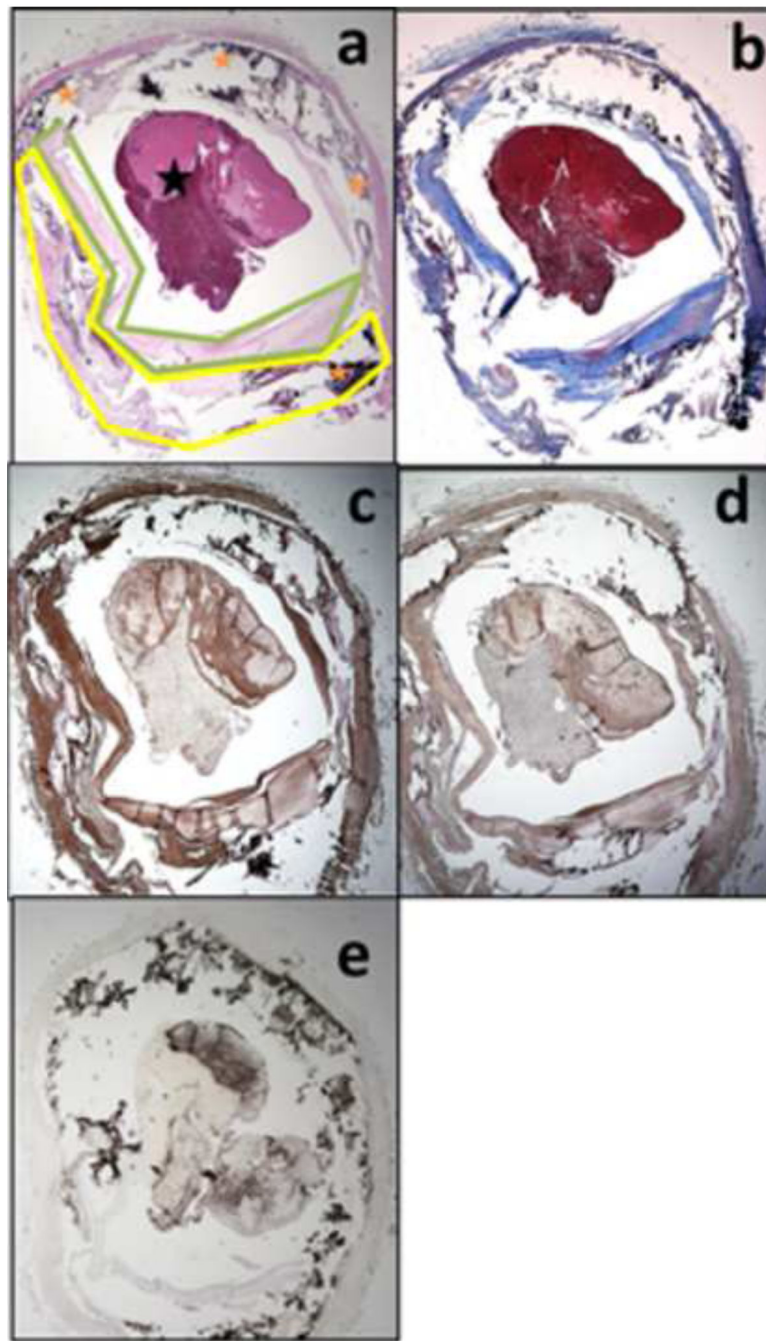


Figure 2. Histopathology of symptomatic left intracranial internal carotid (ICA) plaque Pathological specimens (2x magnification) at the level of the stenosis stained with Hematoxylin & Eosin (a), Trichrome (b), and immunostaining with IL-6 (c), TNF- α (d), and CD68 (counterstained with hematoxylin) (e), which demonstrated plaque components: lipid and loose matrix (yellow outline), fibrous tissue (green outline), calcium (orange star), and post-mortem thrombus (black star).